ISSCR

MiR-203 Interplays with Polycomb Repressive Complexes to Regulate the Proliferation of Neural Stem/Progenitor Cells

Pei-Pei Liu,[1,2] Gang-Bin Tang,[1] Ya-Jie Xu,[1,2] Yu-Qiang Zeng,[1] Shuang-Feng Zhang,[1,3] Hong-Zhen Du,[1] Zhao-Qian Teng,[1,2,*] and Chang-Mei Liu[1,2,*]

[1]State Key Laboratory of Stem Cell and Reproductive Biology, Institute of Zoology, Chinese Academy of Sciences, Beijing 100101, China
[2]Savaid Medical School, University of Chinese Academy of Sciences, Beijing 100049, China
[3]School of Life Sciences, University of Science and Technology of China, Hefei 230027, China
*Correspondence: tengzq@ioz.ac.cn (Z.-Q.T.), liuchm@ioz.ac.cn (C.-M.L.)
http://dx.doi.org/10.1016/j.stemcr.2017.05.007

SUMMARY

The polycomb repressive complexes 1 (PRC1) and 2 (PRC2) are two distinct polycomb group (PcG) proteins that maintain the stable silencing of specific sets of genes through chromatin modifications. Although the PRC2 component EZH2 has been known as an epigenetic regulator in promoting the proliferation of neural stem/progenitor cells (NSPCs), the regulatory network that controls this process remains largely unknown. Here we show that miR-203 is repressed by EZH2 in both embryonic and adult NSPCs. MiR-203 negatively regulates the proliferation of NSPCs. One of PRC1 components, *Bmi1*, is a downstream target of miR-203 in NSPCs. Conditional knockout of *Ezh2* results in decreased proliferation ability of both embryonic and adult NSPCs. Meanwhile, ectopic overexpression of BMI1 rescues the proliferation defects exhibited by miR-203 overexpression or EZH2 deficiency in NSPCs. Therefore, this study provides evidence for coordinated function of the EZH2-miR-203-BMI1 regulatory axis that regulates the proliferation of NSPCs.

INTRODUCTION

Neural stem cells (NSCs) are self-renewing, multipotent cells that have the capability to differentiate into neurons, astrocytes, and oligodendrocytes (Gage, 2000). NSCs are abundant during CNS development and also exist in the adult nervous system of all mammals, including humans (Spalding et al., 2013). NSCs not only provide a model of nervous system development but also have great therapeutic potential for the treatment of CNS injuries and diseases (Dixon et al., 2015; Ruan et al., 2014; Stenudd et al., 2015). A better understanding of molecular mechanisms regulating their behavior, especially self-renewal ability and stemness maintenance, is required to fully exploit the capacity of these cells. The mechanisms underlying the regulation of NSCs proliferation and maintenance of their multipotency have not yet been completely elucidated (Batista et al., 2014; Sher et al., 2008; Ziegler et al., 2015).

Polycomb group (PcG) proteins comprise the Polycomb complexes PRC1 and PRC2 in the nucleus and regulate gene expression levels through histone modifications (Sparmann and van Lohuizen, 2006; Takamatsu-Ichihara and Kitabayashi, 2016). Dysregulation of PcG proteins can contribute to a number of human diseases, most notably cancer (Bracken and Helin, 2009; Margueron and Reinberg, 2011). PRC1 is composed of BMI1, CBXs, RING1 and RING2, and functions as a multi-protein complex to ubiquitinate histone H2A at lysine 119 (uH2A) (Cao et al., 2005; Wang et al., 2004), and to condense chromatin to repress transcription (Francis et al., 2004). PRC2 typically contains EZH1/2, SUZ12, and EED. EZH2 is a his-

tone methyltransferase responsible for catalyzing histone H3 lysine 27 trimethylation (H3K27me3) (Cao et al., 2002; Czermin et al., 2002). EED and SUZ12 are necessary factors for the recruitment of PRC2 to nucleosomes and histone methyltransferase activity (Cao and Zhang, 2004; Margueron et al., 2009). A previous study suggests that PRC1 and PRC2 might coordinate in epigenetic silencing of target genes through some unknown mechanisms (Bracken and Helin, 2009).

PRC1 and PRC2 are important epigenetic regulators in NSPCs. EZH2 is highly expressed in NSPCs, with little protein expression in neurons, which suggests that PcG protein might be involved in stem cell renewal and maintenance (Pereira et al., 2010; Sher et al., 2008; Zhang et al., 2014). In the early developing forebrain, conditional deletion of *Ezh2* results in a shortened period of neuronal production related to lack of precursor cell proliferation and premature NSPC differentiation (Pereira et al., 2010). Meanwhile, in adult NSPCs the deletion of *Ezh2* in NSPCs results in a reduction in progenitor cell proliferation (Hwang et al., 2014; Zhang et al., 2015). Importantly, postnatal NSPCs lacking the PRC1 component BMI1 are defective for proliferation, in part due to the repression of cell-cycle inhibitors encoded by the Ink4a/Arf locus (Molofsky et al., 2003). PRC1 and PRC2 are thought to coordinately maintain the gene expression pattern in different cells (Margueron and Reinberg, 2011).

MicroRNA (miRNA) is a class of non-coding RNAs that also play critical roles in NSPCs (Kawahara et al., 2012; Liu et al., 2010; Nguyen et al., 2015). In cancer cell lines and prostate cancer tissues, there is an inverse correlation

CrossMark
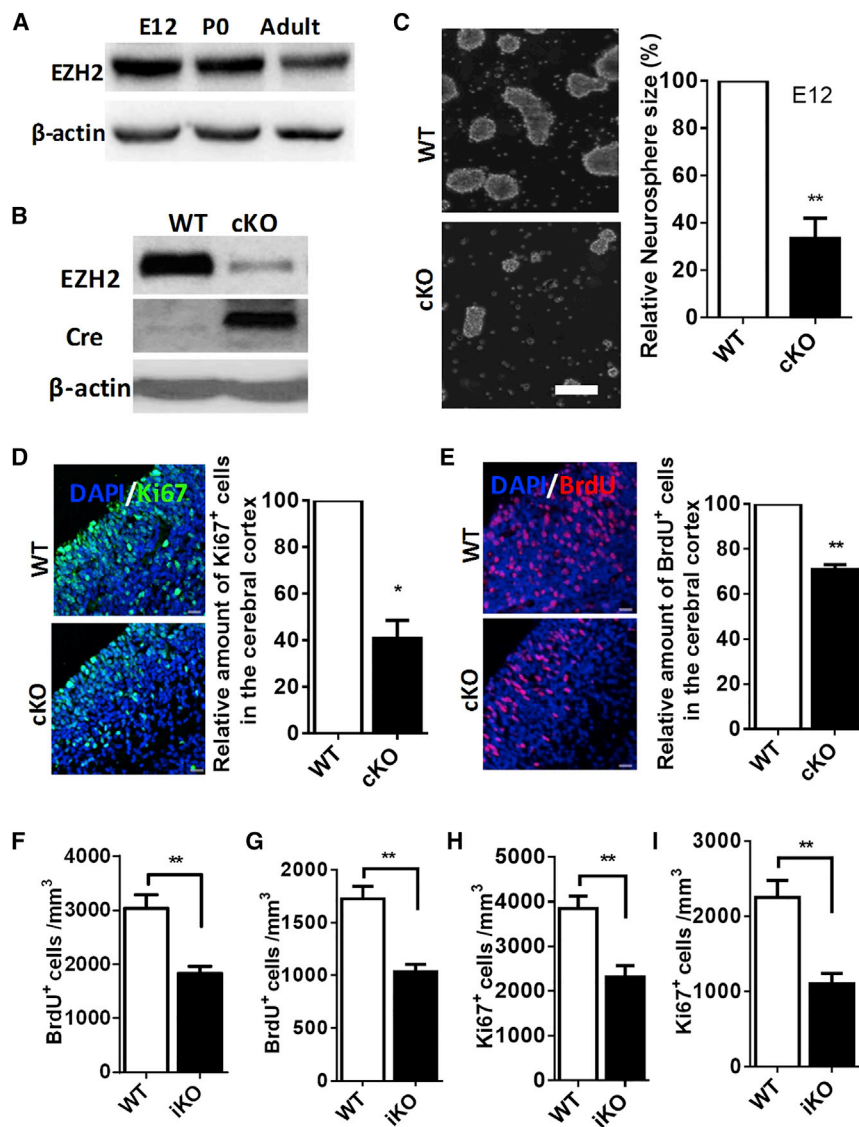
Figure 1. EZH2 Loss of Function Impairs Proliferation of Both Embryonic and Adult NSPCs

(A) Western blot showed that EZH2 was highly expressed in E12, newborn P0, or adult NSPCs.

(B) EZH2 was almost undetectable in the cortex of *Ezh2* cKO mice at E14 by western blot analysis.

(C) Representative images of neurospheres formed by NSPCs isolated from *Ezh2* WT and cKO littermates at E12. The diameters of neurospheres were significantly smaller in cKO mouse-derived cultures. Neurospheres were derived from three different pairs of littermates. Scale bar, 100 μm.

(D) Ki67 immunostaining showed that cell proliferation was decreased in the cerebral cortex of *Ezh2* cKO mice at E14. Scale bar, 30 μm.

(E) Decreased proliferation in the cerebral cortex of *Ezh2* cKO mice at E14 was confirmed by BrdU incorporation assay. Scale bar, 30 μm.

(F) BrdU incorporation assay demonstrated that there were fewer BrdU+ cells in the DG of *Ezh2* iKO mice at 2 months old after tamoxifen injection.

(H) Ki67 staining supported that *Ezh2* iKO mice had fewer proliferating cells in the DG at 2 months old after tamoxifen injection compared with control mice.

(G and I) *Ezh2* iKO mice had significantly declined proliferating cell numbers in the DG even at 6 months old after tamoxifen injection by BrdU incorporation assay (G) and Ki67 staining analysis (I). The brain tissues at the specific time points came from four to six mice.

Mean ± SEM; *p < 0.05, **p < 0.01. See also Figure S1.

between miRNA and PRC protein levels, suggesting a possible model for a coordinated PRC2-PRC1 oncoprotein axis mediated by PRC2-regulated miRNAs (Cao et al., 2011). In this study, we provide the evidence showing that miR-203 is a mediator between PRC2 and PRC1 that modulates NSPC proliferation.

RESULTS

EZH2 Is Highly Expressed in NSPCs but Decreased Rapidly upon Their Differentiation

To explore the functions of EZH2 in NSPCs, we first examined its expression levels during brain development by measuring both mRNA and protein levels of *Ezh2* in NSPCs isolated at different embryonic and postnatal stages. *Ezh2* expression level was detected in NSPCs which were isolated from embryonic day 12 (E12), newborn (postnatal day 0 [P0]), or adult forebrain. We observed that *Ezh2* protein level was highly expressed in NSPCs at E12, P0, and adulthood (Figure 1A). Moreover, once differentiation of embryonic NSPCs was initiated in vitro, both *Ezh2* mRNA and protein levels gradually decreased during NSPC differentiation at days 2, 4, 6, and 8 (Figures S1A and S1B). Downregulation of EZH2 in cortical tissues during development from E15 to adult was then verified by RT-PCR and western blot (Figures S1C and S1D). Previous studies have also shown that EZH2 is highly expressed in NSPCs, with little protein

expression in neurons (Pereira et al., 2010; Sher et al., 2008; Zhang et al., 2014). Therefore, EZH2 may play a pivotal role in maintaining self-renewal and proliferation of NSPCs.

Ezh2 Loss of Function Impairs Proliferation of Both Embryonic and Adult NSPCs

As enriched expression of EZH2 was detected in early stages of brain development, we next tested whether EZH2 affects NSPCs proliferation. First, we performed neurosphere assays for the forebrain NSPCs isolated from $Ezh2^{f/f}$ or $Ezh2^{f/f;Nestin-Cre}$ (EZH2 conditional knockout [cKO]) mice at E12, which were generated by breeding $Nestin-Cre$ mice with $Ezh2^{f/f}$ mice (Figure S1E). As expected, immunoblotting results showed that EZH2 was almost undetectable in EZH2 cKO forebrain tissue at E12 compared with the control group (Figure 1B). Neurosphere assay results showed that EZH2 cKO NSPCs formed fewer and smaller neurospheres than those from wild-type (WT) littermates at E12 (Figure 1C), E14 (Figure S1F), and E17 (Figure S1G).

To confirm the role of $Ezh2$ in the proliferation of embryonic NSPCs, we conducted immunohistochemistry staining of Ki67 on E14 embryo brain sections from EZH2 WT and cKO littermates. As expected, the number of Ki67-positive cells was significantly reduced in the subventricular zone (SVZ) and the ventricular zone (VZ) in EZH2 cKO mice as compared with that of WT mice (Figure 1D). Similar results were also found in the cerebral cortex of E14 embryos by injecting 100 mg/kg 5-bromodeoxyuridine (BrdU) intraperitoneally to pregnant mother mice 2 hr before embryo collection at E14. The EZH2 cKO embryos demonstrated an obvious decrease in BrdU incorporation into the cerebral cortex NSPCs (Figure 1E). These in vitro and in vivo data indicated that EZH2 was an essential regulator to maintain the proliferation status of embryonic NSPCs.

We next examined whether $Ezh2$ loss of function also affects the proliferation ability of NSPCs in the young and older adult mice. As EZH2 cKO homozygous KO mice cannot survive to adulthood and usually die at P15–P20, we then took advantage of $Ezh2^{f/f;Nestin-CreERT2}$ (EZH2 iKO) mice (Figure S1E) to further investigate whether $Ezh2$ is also involved in adult NSPC proliferation. The EZH2 inducible KO (iKO) mice were injected with tamoxifen at 4 weeks of age for a total five times, three times in the first week followed by one injection each of the following 2 weeks (Figure S1H). Real-time PCR and immunoblotting results showed that both mRNA and protein levels of EZH2 were dramatically downregulated after a total of five tamoxifen injections (Figures S1I and S1J). Mice then received a 100 mg/kg BrdU injection 2 hr before analysis at either 2 months or 6 months old (Figure S1H). We observed that BrdU-positive cells significantly decreased in the dentate gyrus (DG) of EZH2 iKO mice compared

with that of WT mice, regardless of whether the mouse was 2 months old (Figures 1F and S1K) or 6 months old (Figures 1G and S1L). Meanwhile, reduced numbers of Ki67$^+$ cells were exhibited in both 2-month-old (Figures 1H and S1M) and 6-month-old (Figures 1I and S1N) EZH2 iKO mice. These data suggested that deletion of $Ezh2$ also impaired the proliferation of young and older adult NSPCs. Therefore, our data suggested that EZH2 may maintain the proliferation ability of NSPCs at all developmental stages in mice.

EZH2-miR-203-Bmi1 Regulatory Axis Exists in NSPCs

As PRC2 provides a substrate for PRC1 recruitment (Margueron and Reinberg, 2011), we next examined the expression levels of PRC1 in EZH2 cKO mice. mRNA level of $Bmi1$, also known as polycomb group RING finger protein 4 (PCGF4), was significantly reduced in EZH2 cKO cortex compared with WT NSPCs at E14 (Figure 2A). In addition, western blot demonstrated that BMI1 protein was also decreased in EZH2 cKO cortex at E14 (Figure 2B).

Increasing evidence has emerged that miRNAs play an important role in regulation of stem cell proliferation, and EZH2 is able to repress miRNA expression (Szulwach et al., 2010). Mouse $Bmi1$ 3′ UTR is 2,148 bp long, and TargetScan (Agarwal et al., 2015) predicted that there are only six binding sites for miRNA families broadly conserved among vertebrates (Table S1). Among these broadly conserved miRNAs, miR-203 has been experimentally validated as a direct regulator of $Bmi1$ in lung cancer (Chen et al., 2015), we hypothesized that EZH2 may also govern $Bmi1$ expression in NSPCs through miR-203. To test this hypothesis, we first examined the expression of miR-203 along with several other miRNAs in EZH2 cKO NSPCs isolated from E12 forebrain and found that the expression of miR-203 was increased in EZH2 cKO NSPCs (Figure 2C). In situ hybridization staining for mature miR-203 confirmed the higher expression of miR-203 in the VZ, SVZ, and cortical plate, but lower expression in the intermediate zone (IZ) in the developing cortex at E14 (Figures 2D and S2A). To further determine whether EZH2 also regulates the expression of miR-203 in adult NSPCs, we acutely manipulated EZH2 expression in adult NSPCs with lentivirus. As expected, we found that acute knockdown of EZH2 in adult NSPCs with lenti-EZH2-short hairpin RNA (shRNA) virus led to increased miR-203 expression (Figure 2E), whereas overexpression of EZH2 led to reduced miR-203 expression (Figure 2F).

EZH2, as one of the PRC2 components, is a histone methyltransferase that plays an essential role in the epigenetic maintenance of the H3K27me3 repressive chromatin mark. We then proceeded to explore whether EZH2 directly regulates miR-203 in NSPCs. We firstly used H3K27me3-specific chromatin immunoprecipitation (ChIP) in isolated
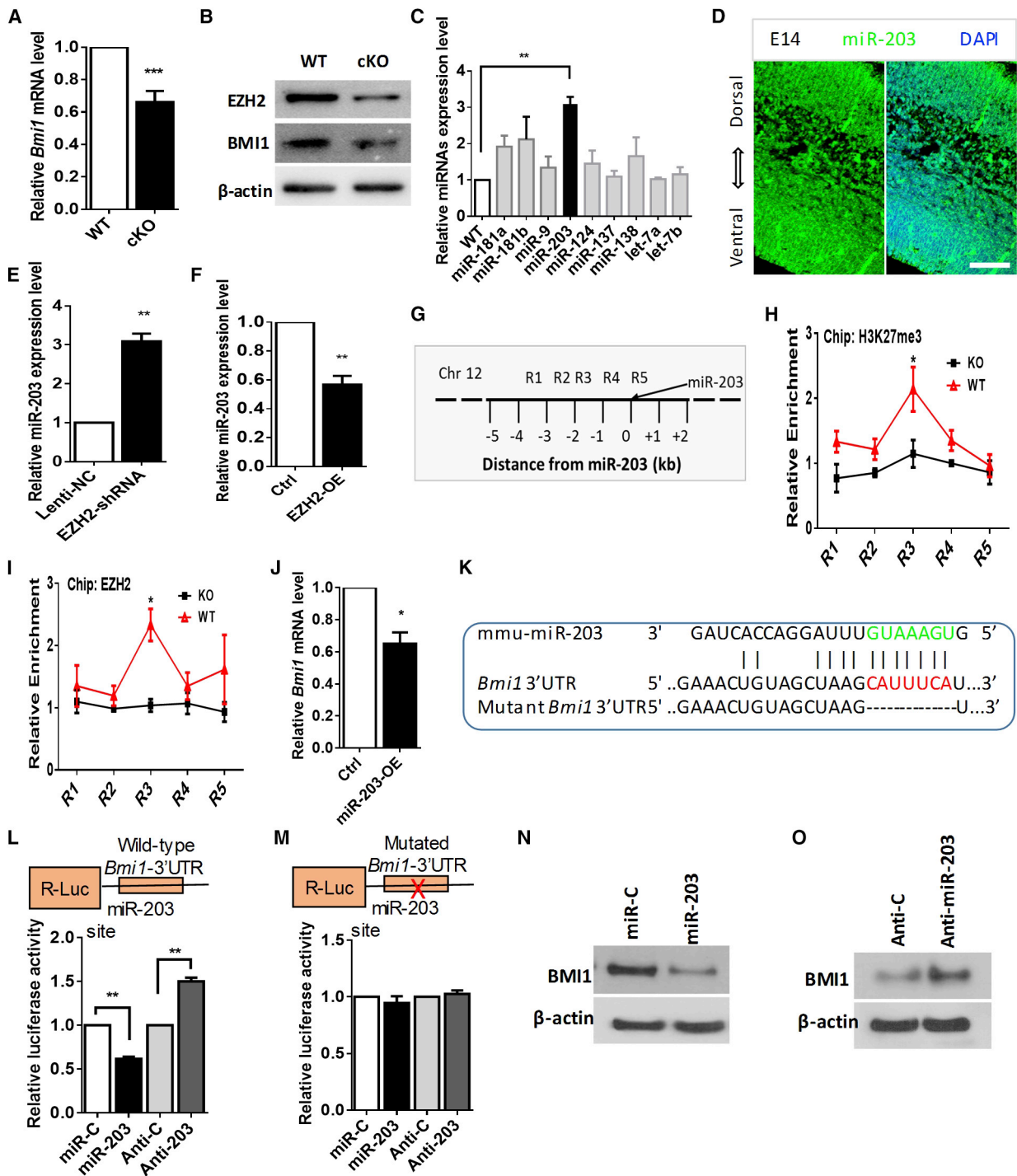
Figure 2. *Bmi1* and miR-203 Are Upregulated in EZH2 cKO Mice, and EZH2-miR-203-BMI1 Regulatory Axis Exists in NSPCs

(A) RT-PCR showed that *Bmi1* mRNA expression was significantly downregulated in the cortex of EZH2 cKO mice at E14. RNA samples were extracted from seven different pairs of littermates.

(B) Western blot showed that the protein expression of *Bmi1* was also significantly reduced in the EZH2 cKO cortex at E14.

(C) Quantification analyses of miRNAs indicated that miR-203 was upregulated in EZH2 cKO embryonic NSPCs at E12.

(D) In situ hybridization for mature miR-203 was present throughout the cortex at E14. Higher expression of miR-203 was observed in the ventricular zone, subventricular zone, and cortical plate, but lower in the intermediate zone in the developing cortex. Scale bar, 100 μm.

(legend continued on next page)

E12 NSPCs from EZH2 WT and cKO littermates, and analyzed the interaction between H3K27me3 and five genomic regions (R1–R5) from 4 kb upstream to 1 kb downstream of the miR-203 gene (Figure 2G) through ChIP followed by the real-time qPCR. Strong enrichment of H3K27me3 in the R3 region of miR-203 was found in EZH2 WT NSPCs relative to in cKO NSPCs (Figure 2H). Again, EZH2-specific ChIP further proved that EZH2 does have a binding site in the R3 region of miR-203 (Figure 2I). Taken together, these results suggested that EZH2 repressed the expression of miR-203 through directly binding to the upstream genomic regions of miR-203 gene in NSPCs.

We found that miR-203 expression was gradually increased during the process of differentiation of cultured adult NSPCs (Figure S2B). Next, we examined whether miR-203 is responsible for the expression levels of endogenous Bmi1 in NSPCs. Our RT-PCR data demonstrated that Bmi1 mRNA expression was robustly reduced after overexpressing miR-203 in adult NSPCs (Figure 2J). Other PRC1 components, Ring 1a and Ring1b, were also reduced under miR-203 overexpression conditions in adult NSPCs (Figures S2C and S2D). To further determine whether Bmi1 is a direct target of miR-203, we used luciferase reporter assay by cloning the 3′ UTR sequence of Bmi1 containing the predicted miR-203 binding site (Figure 2K) into a dual luciferase reporter construct, which allowed us to assess BMI1 protein translation based on luciferase activities. Reporter constructs along with the miR-203 mimics or its inhibitor were transiently transfected into a mouse CNS catecholaminergic cell line (CAD cells). We found that miR-203 overexpression could repress the expression of Renilla luciferase (R-Luc) activity through the Bmi1 3′ UTR, whereas miR-203 inhibitor enhanced the expression of R-Luc (Figure 2L). To further confirm that the binding site within Bmi1 3′ UTR was specific to miR-203, we mutated the binding site of miR-203 on Bmi1 3′ UTR in the R-Luc

reporter, and found that miR-203 mimics or its inhibitor could not affect the mutated Bmi1 3′ UTR R-Luc expression (Figure 2M). Next, we electroporated miR-203 mimics or its inhibitor into isolated adult NSPCs, followed by BMI1 protein analysis by western blot 4 days later. A reduction of BMI1 protein level was found in the miR-203-overexpression group (Figure 2N), while blocking the expression of miR-203 by its inhibitor elevated the protein level of Bmi1 in adult NSPCs (Figure 2O). Taken together, these results suggested that an EZH2-miR-203-BMI1 regulatory axis exists in NSPCs.

MiR-203 Inhibits Proliferation Ability of NSPCs In Vitro and In Vivo

miR-203 expression gradually increased during embryonic cortical development and remained at a relatively high level in the cortex until adulthood (Figure 3A), which indicates that miR-203 may be an inhibitor of NSPC proliferation. We next examined its functions in NSPCs. We created a recombinant lentiviral vector expressing miR-203 (Lenti-miR-203), and a sponge lentiviral vector (lenti-miR-203-sponge) knocking down miR-203, which has nearly 100% infection efficiency, into cultured adult NSPCs as indicated by co-expressing GFP expression (Figure 3B). Our RT-PCR data demonstrated that our constructed lenti-miR-203 sponge virus had efficiency similar to that of anti-miR-203 oligos for knocking down mature miR-203 (Figures S3A and S3B), which could knock down endogenous miR-203 expression. Quantification of BrdU-positive cells after pulse labeling indicated that miR-203 overexpression resulted in a significant decrease, while its knockdown caused a significant increase, in the proportion of BrdU$^+$GFP$^+$ cells compared with NC-control lentivirus-infected adult NSPCs in vitro (Figure 3C). Moreover, overexpression of miR-203 in cultured adult NSPCs resulted in reduced number and size of primary, secondary, and

(E) Knocking down EZH2 with lenti-EZH2-shRNA virus in cultured adult NSPCs led to increased expression of miR-203 in vitro.
(F) Conversely, overexpression of EZH2 with lentivirus led to decreased expression of miR-203 in adult NSPCs.
(G) Schematic of the 4-kb genomic regions (R1–R5) proximal to the miR-203 gene on chromosome 12 that were analyzed in the ChIP experiment.
(H) RT-PCR data showed that there was an enrichment of H3K27me3 in the R3 genomic region of the miR-203 locus in E12 NSPCs.
(I) RT-PCR data showed that there was an enrichment of the binding site of EZH2 in the R3 genomic region of the miR-203 locus in E12 NSPCs.
(J) Quantification analyses of mRNAs indicated that Bmi1 was downregulated in miR-203 overexpression embryonic NSPCs at E12.
(K) An miR-203 target site was predicted in the Bmi1 3′ UTR by TargetScan. The seed sequence of miR-203 is shown in green. The mutant Bmi1 3′ UTR used in luciferase assay has a 7-bp deletion of the miR-203 target site (in red).
(L) R-Luc activity assay of CAD cells that were co-transfected the luciferase reporter containing the full-length Bmi1 WT 3′ UTR with miR-203 mimics or its inhibitor.
(M) Mutation of the miR-203 targeting site in the Bmi1 3′ UTR abolished the regulation of luciferase activity by miR-203 mimics or its inhibitor.
(N) Western blot supported that Bmi1 protein expression was downregulated in E12 NSPCs under miR-203 overexpression.
(O) Overexpression of the miR-203 inhibitors led to increased endogenous Bmi1 protein level in cultured E12 NSPCs.
n = 3 or 4 independent experiments. Mean ± SEM; *p < 0.05, **p < 0.01, ***p < 0.001. See also Figure S2.
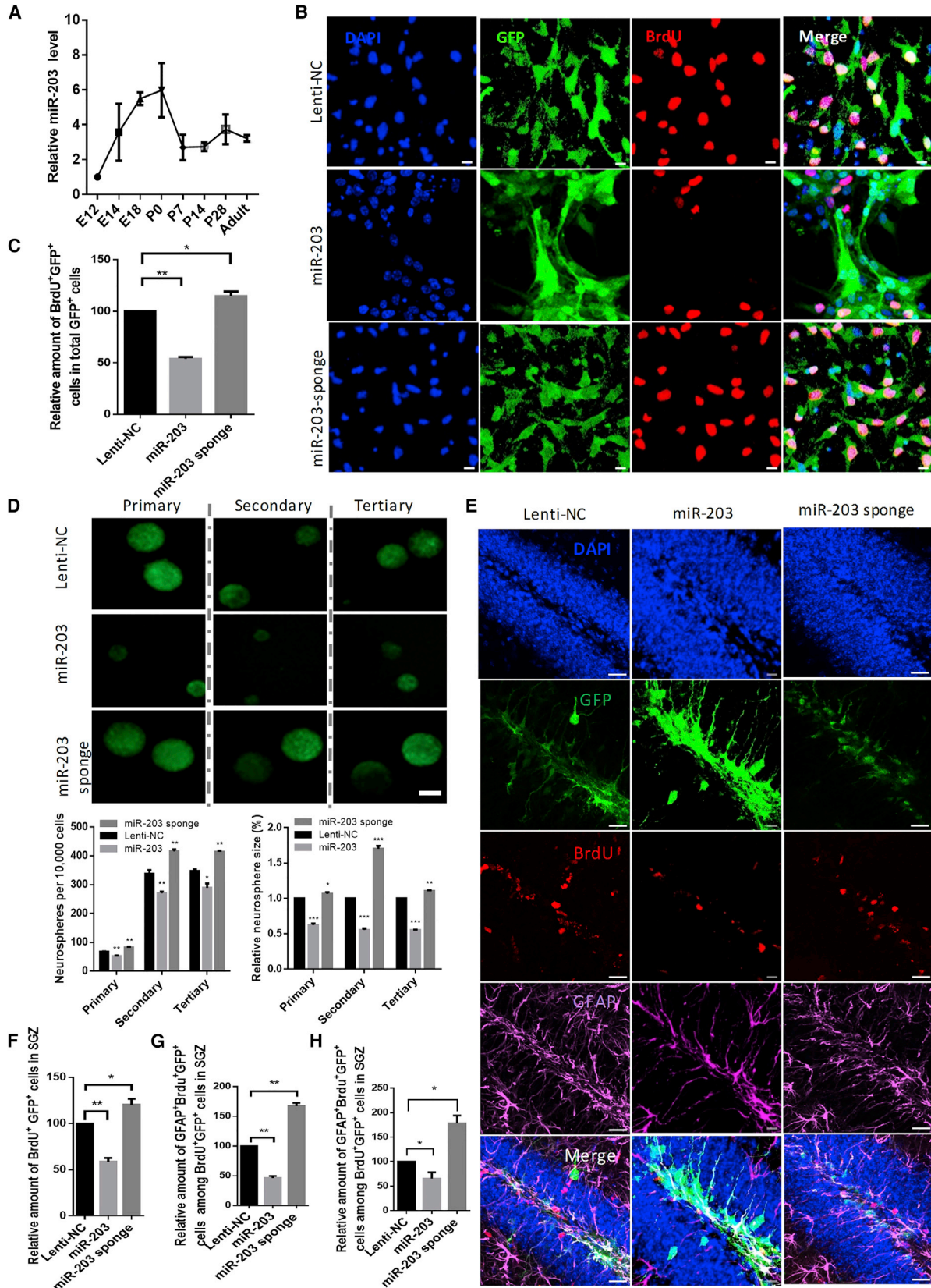
(legend on next page)

tertiary neurospheres, while the number and size of neurospheres were significantly increased in miR-203 inhibition (sponge) treatment (Figure 3D). There were no detectable signals of caspase-3 on cultured NSPCs which were infected with lenti-miR-203 or lenti-miR-203-sponge, indicating miR-203 had no effect on cell death of NSPCs (Figure S4).

To examine whether miR-203 impairs the proliferation of adult NSPCs in vivo, we took advantage of the persistent neurogenesis in the DG of the postnatal hippocampus, which recapitulates the neurogenic process during development. Recombinant lenti-miR-203 or lenti-miR-203-sponge virus was injected stereotactically into the right DG, and control lentivirus (lenti-NC) was grafted into the left DG of the same mouse. To assess proliferation of lentivirus-labeled NSPCs, we also injected mice with BrdU immediately after the surgery. At 1 week after viral grafting, we quantified the amount of BrdU$^+$GFP$^+$ cells in the subgranular zone (SGZ), and found a 42.3% reduction of BrdU$^+$GFP$^+$ cells in lenti-mR-203 grafted SGZ and a notable 20.5% increase in the number of BrdU$^+$GFP$^+$ cells in lenti-mR-203-sponge-GFP grafted SGZ relative to control lenti-NC grafted SGZ (Figures 3E and 3F). We then performed immunostaining for BrdU (red) and glial fibrillary acidic protein (GFAP) (purple) to analyze the amount of adult NSCs in SGZ at either 7 days in vitro (DIV 7) or DIV 14. Quantification of GFAP$^+$BrdU$^+$GFP$^+$ cells indicated a big reduction of GFAP$^+$BrdU$^+$GFP$^+$ cells in the lenti-miR-203 grafted SGZ and a significant increase of GFAP$^+$BrdU$^+$GFP$^+$ cells in the lenti-miR-203-sponge grafted SGZ at both DIV 7 (Figure 3G) and DIV 14 (Figure 3H) relative to control lentivirus grafted SGZ. Considering that some of GFAP$^+$ NSPCs may differentiate into astrocytes (Bonaguidi et al., 2011) and miR-203 promotes astrogliogenesis (Figures S3D, S5C, and S5D), the reduced amount of cycling NSPCs

we observed might be overestimated in the lenti-miR-203 grafted SGZ, and the increased number of cycling NSPCs might be underestimated in the lenti-miR-203-sponge grafted SGZ. Therefore, these data suggested that miR-203 could also impair the proliferation of adult NSPCs in vivo.

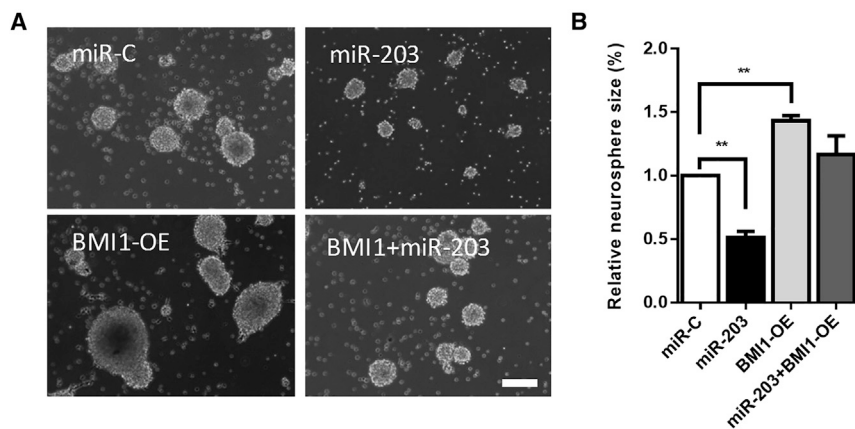### BMI1 Rescues the Phenotype of miR-203 Overexpression in Adult NSPCs

To determine whether BMI1 could rescue the proliferation deficits of miR-203 overexpression in adult NSPCs, we electroporated lenti-NC-GFP, miR-203 mimics, lenti-BMI1-OE, or both lenti-BMI1-OE and miR-203 mimics into adult NSPCs that were isolated from the forebrain of adult C57BL/6 mice. Adult NSPCs with elevated expression of miR-203 formed 50% fewer and much smaller neurospheres compared with the lenti-NC-GFP treatment (Figures 4A and 4B). As expected, overexpression of BMI1 led to a significant increase in both size and number of neurospheres relative to the control (Figures 4A and 4B). However, adult NSPCs that were co-electroporated with lenti-BMI1-OE and miR-203 mimics had similar size and number of neurospheres compared with the control (Figures 4A and 4B). These data suggested that restoration of BMI1 expression in miR-203-overexpressed adult NSPCs could rescue their proliferation ability.

BMI1 Partially Rescues NSPC Proliferation Deficits Associated with EZH2 Deficiency

As *Bmi1* expression level was downregulated in EZH2 cKO cortex, we next investigated whether *Bmi1* gain of function could rescue NSPC proliferation deficits in EZH2 cKO mice. *Bmi1* protein expression was significantly reduced in E12 NSPCs of EZH2 cKO mice (Figure 5A), and a notable reduction of *Bmi1* protein was also found in *Ezh2$^{f/f}$* embryonic

---

Figure 3. miR-203 Regulates the Proliferation of Adult NSPCs

(A) MiR-203 was upregulated during embryonic cortical development and kept at a relatively high level to adult.

(B and C) Infection of adult NSPCs with lenti-miR-203 or lenti-miR-203 sponge virus, which was co-expressing GFP under the CMV promoter, allowing us to track infected cells (B, green). The proliferation ability of adult NSPCs was assessed by BrdU labeling (B, red). Scale bars, 10 μm. Percentage of BrdU$^+$ cells was reduced from 46% to 25% in adult NSPCs that were infected with Lenti-miR-203 virus, compared with control shRNA (Lenti-NC) virus-infected adult NSPCs (C).

(D) Morphological examination of adult NSPCs neurospheres that appeared 7 days after initial plating showed that overexpression of miR-203 in cultured adult NSPCs resulted in reduced number and size of primary, secondary, and tertiary neurospheres, while increased number and size of neurospheres was observed in miR-203 inhibition (sponge) treatment. Scale bar, 50 μm.

(E and F) Lenti-miR-203, lenti-miR-203-sponge, or control lenti-NC viruses were grafted into the SGZ of adult hippocampus (E). Note that GFP expression was largely confined to the dentate area. Immunostaining for BrdU (red) and GFAP (purple) was used to identify adult NSCs in SGZ in the hippocampus. Scale bar, 30 μm. Quantification of BrdU$^+$GFP$^+$ cells (F) indicated a large reduction of BrdU$^+$GFP$^+$ cells in the lenti-miR-203 grafted SGZ, and a significant increase of BrdU$^+$GFP$^+$ cells in the lenti-miR-203-sponge grafted SGZ at DIV 7 relative to control lentivirus grafted SGZ, indicating that miR-203 inhibited, but loss of miR-203 elevated, the proliferation of adult NSPCs.

(G and H) Meanwhile, the percentages of adult NSCs (GFAP$^+$BrdU$^+$GFP$^+$) among all BrdU$^+$GFP$^+$ cells in SGZ at DIV 7 (G) and DIV 14 (H) were significantly reduced in miR-203 overexpression group, but increased in miR-203 sponge group, indicating that miR-203 prevented proliferation of adult NSPCs.

n = 4 independent experiments or different pairs of littermates. Mean ± SEM; *p < 0.05, **p < 0.01, ***p < 0.001. See also Figures S3 and S4.

Figure 4. BMI1 Rescues the Phenotype of miR-203 Overexpression in Adult NSPCs

(A) Representative images of adult NSPC proliferation under the overexpression condition of miR-203, BMI1, or both. Scale bar, 100 μm.

(B) MiR-203-electroporated adult NSPCs exhibited smaller neurospheres compared with miR-C-electroporated cells. Overexpression of BMI1 in adult NSPCs resulted in bigger neurospheres compared with miR-C-treated adult NSPCs. Restoration of BMI1 expression in miR-203-overexpression adult NSPCs rescued their proliferation ability.

n = 4 independent experiments. Mean ± SEM; **p < 0.01.

cortex NSPCs at 4 days after infecting with lenti-*Cre* virus (Figure 5B). We then isolated E12 NSPCs from EZH2 cKO and WT littermates, and electroporated NSPCs with lenti-BMI1-OE or lenti-NC plasmids. Our results indicated that the recovery of BMI1 expression in EZH2 cKO NSPCs promoted their proliferation ability by generating more and larger neurospheres (Figures 5C and 5D), but fewer and smaller neurospheres than those of WT, which suggests that restoration of BMI1 in EZH2 cKO NSPCs partially rescue the proliferation ability exhibited by EZH2 deficits. Therefore, other downstream targets might also contribute to the proliferation deficits in EZH2 cKO NSPCs.

DISCUSSION

NSPCs and their derivatives are thought to have tremendous potential in the development of cell replacement therapies for many neurodegenerative disorders, because to date there are no neuroprotective therapies that can prevent cell loss and because substantial cell loss most often has already occurred before diagnosis (Hagg, 2005; Lindvall et al., 2004, 2012). As endogenous NSPCs are thought to be a potential source of stem cells for treating neurological diseases (Dietrich and Kempermann, 2006; Stenudd et al., 2015; Yu et al., 2016), a better understanding of the regulation mechanisms underlying NSPC proliferation and differentiation should lead to more selective and effective stem cell therapy (Hagg, 2005; Stenudd et al., 2015).

The epigenetic modification of developmental genes, including alterations in DNA methylation, histone modifications, PcG, and non-coding RNA expression, which are passed on through successive cell divisions, has been suggested as one of the major mechanisms determining the fate of NSPCs (Mohamed Ariff et al., 2012). In our study, we provide the evidence for coordinated functions of PcG

proteins, EZH2 and BMI1, in regulating NSPC proliferation, and identified miR-203 as the inter-regulator between EZH2 and BMI1 in NSPCs.

We demonstrate here that EZH2 is highly expressed in NSPCs but decreased upon differentiation, whereas the level of miR-203 is increased upon differentiation. EZH2 has been reported as an important epigenetic regulator not only in promoting proliferation but also in controlling fate choices of NSPCs in the cerebral cortex (Pereira et al., 2010). EZH2 promotes the amplification of adult NSPCs and progenitor cells through the Pten-Akt-mTOR signaling pathway (Zhang et al., 2014). Consistent with these studies, we show here that conditional knockout of *Ezh2* has a significant effect on impairing proliferation of embryonic NSPCs and that EZH2 is also essential for NSPC maintenance in adult mice.

miR-203 has been previously reported as an important tumor repressor in breast and prostate cancers (Cao et al., 2011), and *Bmi1* has been validated as a direct target of miR-203 in controlling cell proliferation and proliferation of esophageal cancer stem-like cells (Yu et al., 2014). Furthermore, several other studies provide evidence showing that *Bmi1* plays a critical role in the maintenance of NSPC multipotency and proliferation in the forebrain (Fasano et al., 2009), and miR-203 has been previously suggested to play a unique role during the entire process of epidermal development by extending its spectrum of action from the early commitment of human embryonic stem cells to ultimate differentiation of the organ (Nissan et al., 2011). In this study, we provide evidence that the EZH2-miR-203-BMI1 regulatory axis exists in NSPCs. EZH2 epigenetically represses miR-203 expression, and conditional KO of EZH2 results in miR-203 upregulation in NSPCs. Overexpression of miR-203 downregulates BMI1 expression in NSPCs, which inhibits the proliferation ability of NSPCs. Even though *Ring1a* and *Ring1b* are not
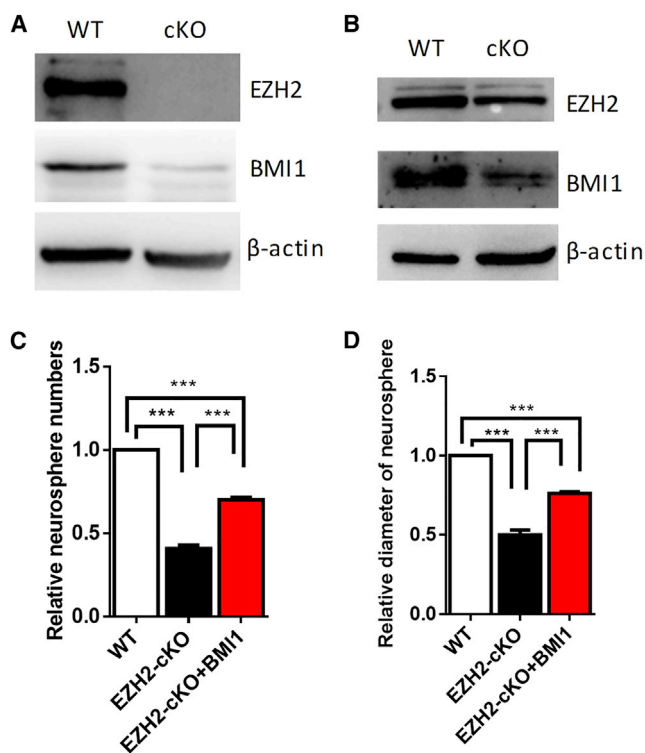
Figure 5. BMI1 Partially Rescues Embryonic NSPC Proliferation Deficits Associated with EZH2 Deficiency

(A) Western blot showed that the protein expression of *Bmi1* was significantly reduced in the embryonic forebrain of EZH2 cKO mice compared with that of WT mice. β-actin was used as an internal control.

(B) Reduced *Bmi1* protein level was also observed in embryonic *Ezh2*$^{f/f}$ NSPCs infected by lenti-*Cre* virus.

(C) Exogenous overexpression of *Bmi1* in *Ezh2*$^{f/f;Nestin-Cre}$ E12 NSPCs resulted in more neurospheres as measured by neurosphere numbers.

(D) Exogenous overexpression of *Bmi1* in *Ezh2*$^{f/f;Nestin-Cre}$ E12 NSPCs resulted in larger neurospheres as measured by neurosphere diameters.

n = 3 independent experiments. Mean ± SEM; ***p < 0.001.

predicted targets of miR-203, their mRNA levels were also significantly downregulated in miR-203 overexpression NSPCs in the present study. However, their relationship and roles in NSPCs are currently unknown. Future studies on roles of *Ring1a*, *Ring1b*, and other epigenetic regulators will give us a better understanding of the complex network regulating NSPCs.

The role of PRC2 in stem cell fate is still controversial. Gene expression on EED[null] and EZH2[null] ES cells suggested that PRC2 might not be required for the maintenance of embryonic stem cell pluripotency (Chamberlain et al., 2008; Shen et al., 2008). In contrast, several other studies have demonstrated that PRC2 plays an important role in stem

cell fate. Overexpression of *Ezh2* in embryonic stem cells inhibits astrocyte differentiation but promotes oligodendrocyte differentiation (Sher et al., 2008). Deletion of *Ezh2* at E12 disrupts cortical neurogenesis and alters the timing of cortical development (Pereira et al., 2010), and deletion of *Ezh2* in adult NSPCs results in the long-term decrease of neuron production in vivo (Zhang et al., 2014). We found that the EZH2-miR-203-BMI1 regulatory axis might also play important roles in regulating the differentiation of NSPCs. The luciferase analysis demonstrated that miR-203-transfected NSPCs exhibited increased activities of transfected *NeuroD1*-promoter-driven firefly luciferase (Figure S3C) and *GFAP*-promoter driven firefly luciferase (Figure S3D), which suggested that miR-203 promoted neuronal differentiation capacity. MiR-203 gain and loss of function in NSPCs further proved that miR-203 enhanced neuronal differentiation both in vitro (Figures S5A and S5B) and in vivo (Figures S5E and S5F). *Bmi1* is expressed in NSPCs, and *Bmi1*$^{-/-}$ mice present more astrocytes at birth and a generalized gliosis at P30 (Zencak et al., 2005). Consistent with this, we observed that *Bmi1* was robustly downregulated in miR-203-overexpressed NSPCs and miR-203-overexpressed embryonic NSPCs differentiated into more GFAP-positive astrocytes, while miR-203 downregulated embryonic NSPCs differentiated into fewer GFAP-positive astrocytes (Figures S5C and S5D). A key question that remains is whether the controversial findings on the role of PRC2 in stem cell pluripotency are related to the stemness status and different types of stem cells.

As PcG proteins and miRNAs are usually co-expressed in many cell types or cancer tissues, such as keratinocytes (Eckert et al., 2011; Yi et al., 2008), hematopoietic stem cells (Takamatsu-Ichihara and Kitabayashi, 2016), hepatocellular carcinoma (Yonemitsu et al., 2009), lung cancer (Chen et al., 2015; Jin et al., 2013), breast cancer (Ru et al., 2011; Yu et al., 2012), and prostate cancer (Viticchie et al., 2011), it will be of interest to elucidate the complicated regulatory network involving multiple epigenetic factors that are responsible for determining cell fate and balancing the proliferation and differentiation of different cell types in future studies. The detailed regulatory network involving PcG proteins and other epigenetic factors that are responsible for altered NSPC behaviors will provide critical insights into the cellular control of NSPC proliferation and fate choices, and might lead us to find new therapeutic strategies for the treatment of neurological diseases.

EXPERIMENTAL PROCEDURES

Animals

Mice we used were on a C57BL6 background. The *Ezh2*$^{f/f}$ mouse (MMRRC Strain ID 15499) was crossed with *Nestin-Cre* mouse (Jax Stock No. 003771) to generate *Ezh2*$^{f/f;Nestin-Cre}$ conditional

knockout mice (EZH2 cKO). The *Ezh2^{f/f}* mouse was crossed with *Nestin-CreERT2* mouse (Jax Stock No. 016261) to generate EZH2 ^{f/f;Nestin-CreERT2} inducible knockout mice (EZH2 iKO). All the mice experiments were approved by the Animal Committee of the Institute of Zoology, Chinese Academy of Sciences.

Self-Renewal, Proliferation, and Differentiation Analyses of Cultured NSPCs

Isolation of embryonic NSPCs from E12, E14, E17, and P0 forebrain was performed as previously described (Liu et al., 2013a; Nakashima et al., 2001). For isolating adult NSPCs, dentate gyrus from 8- to 12-week-old mouse brain was harvested and digested according to the published methodologies (Guo et al., 2011, 2012; Liu et al., 2013a). The total number and size of spheres that formed in each uncoated 35-mm dish were analyzed in DIV 7 culture. Neurosphere self-renewal assays were performed by dissociating neurospheres in bulk and reculturing the cells at a constant density of 10,000 cells per well in uncoated 24-well culture plates. With a minimum cutoff of 40 μm in diameter, the number and size of secondary or tertiary spheres were measured after 7 DIV. For the *Bmi1* rescue experiments, we use electroporation with *Bmi1* overexpression plasmid. After electroporation, the cells were plated onto uncoated 35-mm dishes. Fresh medium was added to the culture dishes every other day. We counted the neurospheres formed after 7 days of culture. Proliferation and differentiation of NSPCs were analyzed using our previously published method (Guo et al., 2011; Liu et al., 2010). We used only early-passage cells and comparable passage numbers of WT and KO cells. For each experiment, at least triplicate wells of cells were analyzed. At least three independent experiments (n = 3) were performed and used for each statistical analysis (for details, see Supplemental Experimental Procedures).

Lentiviral Constructs

The U6-shRNA lentiviral construct was used to insert mature miR-203 sequence driven by U6 promoter and GFP reporter gene driven by CMV promoter (Jessberger et al., 2009; Lie et al., 2005; Liu et al., 2010). PCR-based generation of miR-203 driven by a U6 promoter was done using a PCR Shagging approach as previously described (Liu et al., 2013a). For knockdown of miR-203, an miR-203-sponge was designed using a bulge design method based on a published paper (Liu et al., 2013a). Binding sites for miRNA-203 were complementary in the seed region with a bulge at positions 9–12 to prevent RNA interference-type cleavage and degradation of the sponge RNA. EZH2 overexpression lentiviral construct (lenti-EZH2-OE) was made by integrating the PCR product of human EZH2 open reading frame sequence into the pCD511B-copGFP vector (Youbio) at the NheI/BamHI sites. All vectors were verified by DNA sequencing before use. Lentivirus production and lentiviral grating in vivo was performed as described previously (Guo et al., 2011; Jessberger et al., 2009; Lie et al., 2005; Liu et al., 2010). For details, see Supplemental Experimental Procedures.

Fluorescence In Situ Hybridization

Fluorescence in situ hybridization (FISH) of mature miR-203 was performed on 10-μm-thick frozen sections of 4% paraformaldehyde-fixed E14 brains using an LNA probe, based on previously described methods (Liu et al., 2010; Silahtaroglu et al., 2007). Slides were hybridized with 2.5 pmol of miR-203 or scrambled probe (Exiqon) diluted in 100 μL of hybridization mixture for 1 hr at 65°C, and the FISH signals were detected using the tyramide signal amplification system according to the manufacturer's instructions (PerkinElmer).

Immunocytochemistry and Immunostaining

Immunocytochemistry and immunostaining were conducted according to published approaches (Guo et al., 2011; Liu et al., 2010, 2013a). For immunostaining cultured cells, anti-neuron-specific type β-III tubulin (Biolegend, #801202; 1:1,000), anti-glial fibrillary acidic protein (Millipore, MAB377; 1:1,000), anti-BrdU (Abcam, ab6326; 1:2000), and anti-cleaved caspase 3 (Cell Signaling, #9664; 1:200) were used as the primary antibodies. For immunohistochemistry staining, the primary antibodies used were as follows: anti-Ki67 (Thermo Fisher, RM9106; 1:1,000), anti-BrdU (Abcam, ab6326; 1:1,000), and anti-DCX (Cell Signaling, #4604; 1:500). The secondary antibodies conjugated to Alexa Fluor 488 or 594 with a concentration of 1:500 were used at room temperature. To analyze the amount of BrdU^+GFP^+, or BrdU^+DCX^+GFP^+ cells in the DG, we used one in six series of 40-μm brain sections starting at beginning of hippocampus (relative to bregma, −1.5 mm) to the end of hippocampus (relative to bregma, −3.5 mm). For details, see Supplemental Experimental Procedures.

Tamoxifen Induction and BrdU Labeling

Tamoxifen (Sigma-Aldrich) was administered at a dose of 180 mg/kg intraperitoneally for a total five times in 3 consecutive weeks. Mice were intraperitoneally injected with 100 mg/kg BrdU (Sigma-Aldrich), and killed 2 hr later to quantify BrdU-positive cells for proliferation analysis.

Western Blotting

Cells, cortex, or hippocampus tissues were dissected from mouse brains under ice-cold saline, pooled, and lysed in ice-cold RIPA buffer (Beyotime, P0013B). Protein samples were separated on 8%–12% SDS-PAGE gels (Bio-Rad) and transferred to polyvinylidene fluoride membranes (Millipore). The membranes were blocked in 5% milk in TBS-T (Tris-buffered saline with 0.05% Tween 20) and incubated with primary antibodies at 4°C overnight. As the primary antibodies, we used monoclonal antibody EZH2 (Cell Signaling, #5246s; 1:1,000), H3K27me3 (Millipore, #7-449; 1:1,000), monoclonal antibody BMI1 (Millipore, 05-637; 1:1,000), monoclonal antibody RING1B (active motif, #39663; 1:1,000), anti-Cre (Millipore, MAB3120; 1:1,000), and monoclonal antibody β-actin (Sigma, A5441; 1:5,000). As the secondary antibodies, we used horseradish peroxidase (HRP)-linked goat anti-mouse or HRP-linked goat anti-rabbit. The immunoreactive products were detected with enhanced chemiluminescence reagent (ECL, Pierce).

Real-Time PCR

Real-Time PCR assay was conducted according to the manufacturer's instructions (for details, see Supplemental Experimental Procedures).

Bmi1 3′ UTR Dual Luciferase Assays

The 3′ UTR sequences of *Bmi1* mRNA were PCR-amplified from mouse cDNA. The sequences of primers for *Bmi1* are: forward sequence, 5′-GCA GAT ACC CAT AAC CTA-3′; reverse sequence, 5′-CAA CAC TTA CAA TGG GAC T-3′. The miR-203 target site in the *Bmi1* 3′ UTR was deleted using the PCR method (Rivetti di Val Cervo et al., 2012). The mutation was then verified by DNA sequencing. The constructs together with the miR-203 mimics or inhibitor were co-transfected into CAD cells using Lipofectamine 2000 transfection reagent (Invitrogen). Luciferase activities were measured using the dual luciferase reporter system (Promega) following the manufacturer's instructions, and the activity of Renilla-Luc reporter was normalized to the activity of the internal control Firefly-Luc to minimize experimental variability.

Chromatin Immunoprecipitation

ChIP was performed as described previously (Liu et al., 2013a, 2010, 2013b). Primer sequences spaced at 1-kb intervals spanning from 4 kb upstream to 1 kb downstream of mmu-miR-203 were designed, and DNA relative enrichment was determined by taking the absolute quantity ratios of specific to nonspecific IPs (normal rabbit immunoglobulin G [IgG] only), IP/IgG, and normalizing to a control genomic region that was not enriched in specific IPs relative to nonspecific IPs. For details, see Supplemental Experimental Procedures.

Statistical Analysis

For statistical analyses, ANOVA and unpaired two-tailed Student's t tests were performed using SPSS statistical software (SPSS V23; IBM), and the data presented as mean ± SEM. Probabilities of $p < 0.05$ were considered statistically significant.

SUPPLEMENTAL INFORMATION

Supplemental Information includes Supplemental Experimental Procedures, five figures, and one table and can be found with this article online at http://dx.doi.org/10.1016/j.stemcr.2017.05.007.

AUTHOR CONTRIBUTIONS

P.-P.L., Z.-Q.T., and C.-M.L.: conception and design, collection and assembly of data, data analysis and interpretation, manuscript writing, and final approval of manuscript. G.-B.T., Y.-J.X., Y.-Q.Z., S.-F.Z., and H.-Z.D.: collection and assembly of data.

REFERENCES

Agarwal, V., Bell, G.W., Nam, J.W., and Bartel, D.P. (2015). Predicting effective microRNA target sites in mammalian mRNAs. Elife *4*, e05005.

Batista, C.E.M., Mariano, E.D., Marie, S.K.N., Teixeira, M.J., Morgalla, M., Tatagiba, M., Li, J., and Lepski, G. (2014). Stem cells in neurology - current perspectives. Arq. Neuropsiquiatr. *72*, 457–465.

Bonaguidi, M.A., Wheeler, M.A., Shapiro, J.S., Stadel, R.P., Sun, G.J., Ming, G.L., and Song, H. (2011). In vivo clonal analysis reveals self-renewing and multipotent adult neural stem cell characteristics. Cell *145*, 1142–1155.

Bracken, A.P., and Helin, K. (2009). Polycomb group proteins: navigators of lineage pathways led astray in cancer. Nat. Rev. Cancer *9*, 773–784.

Cao, R., and Zhang, Y. (2004). SUZ12 is required for both the histone methyltransferase activity and the silencing function of the EED-EZH2 complex. Mol. Cell *15*, 57–67.

Cao, R., Wang, L.J., Wang, H.B., Xia, L., Erdjument-Bromage, H., Tempst, P., Jones, R.S., and Zhang, Y. (2002). Role of histone H3 lysine 27 methylation in polycomb-group silencing. Science *298*, 1039–1043.

Cao, R., Tsukada, Y., and Zhang, Y. (2005). Role of *Bmi-1* and *Ring1A* in H2A ubiquitylation and Hox gene silencing. Mol. Cell *20*, 845–854.

Cao, Q., Mani, R.S., Ateeq, B., Dhanasekaran, S.M., Asangani, I.A., Prensner, J.R., Kim, J.H., Brenner, J.C., Jing, X.J., Cao, X.H., et al. (2011). Coordinated regulation of polycomb group complexes through microRNAs in cancer. Cancer Cell *20*, 187–199.

Chamberlain, S.J., Yee, D., and Magnuson, T. (2008). Polycomb repressive complex 2 is dispensable for maintenance of embryonic stem cell pluripotency. Stem Cells *26*, 1496–1505.

Chen, T.F., Xu, C., Chen, J., Ding, C., Xu, Z.L., Li, C., and Zhao, J. (2015). MicroRNA-203 inhibits cellular proliferation and invasion by targeting *Bmi1* in non-small cell lung cancer. Oncol. Lett. *9*, 2639–2646.

Czermin, B., Melfi, R., McCabe, D., Seitz, V., Imhof, A., and Pirrotta, V. (2002). Drosophila enhancer of Zeste/ESC complexes have a histone H3 methyltransferase activity that marks chromosomal polycomb sites. Cell *111*, 185–196.

Dietrich, J., and Kempermann, G. (2006). Role of endogenous neural stem cells in neurological disease and brain repair. Adv. Exp. Med. Biol. *557*, 191–220.

Dixon, K.J., Theus, M.H., Nelersa, C.M., Mier, J., Travieso, L.G., Yu, T.S., Kernie, S.G., and Liebl, D.J. (2015). Endogenous neural stem/progenitor cells stabilize the cortical microenvironment after traumatic brain injury. J. Neurotrauma *32*, 753–764.

Eckert, R.L., Adhikary, G., Rorke, E.A., Chew, Y.C., and Balasubramanian, S. (2011). Polycomb group proteins are key regulators of keratinocyte function. J. Invest. Dermatol. *131*, 295–301.

Fasano, C.A., Phoenix, T.N., Kokovay, E., Lowry, N., Elkabetz, Y., Dimos, J.T., Lemischka, I.R., Studer, L., and Temple, S. (2009). *Bmi-1* cooperates with Foxg1 to maintain neural stem cell self-renewal in the forebrain. Genes Dev. *23*, 561–574.

Francis, N.J., Kingston, R.E., and Woodcock, C.L. (2004). Chromatin compaction by a polycomb group protein complex. Science *306*, 1574–1577.

Gage, F.H. (2000). Mammalian neural stem cells. Science *287*, 1433–1438.

Guo, W.X., Zhang, L., Christopher, D.M., Teng, Z.Q., Fausett, S.R., Liu, C.M., George, O.L., Klingensmith, J., Jin, P., and Zhao, X.Y. (2011). RNA-binding protein FXR2 regulates adult hippocampal neurogenesis by reducing noggin expression. Neuron *70*, 924–938.

Guo, W., Patzlaff, N.E., Jobe, E.M., and Zhao, X. (2012). Isolation of multipotent neural stem or progenitor cells from both the dentate gyrus and subventricular zone of a single adult mouse. Nat. Protoc. *7*, 2005–2012.

Hagg, T. (2005). Molecular regulation of adult CNS neurogenesis: an integrated view. Trends Neurosci. *28*, 589–595.

Hwang, W.W., Salinas, R.D., Siu, J.J., Kelley, K.W., Delgado, R.N., Paredes, M.F., Alvarez-Buylla, A., Oldham, M.C., and Lim, D.A. (2014). Distinct and separable roles for EZH2 in neurogenic astroglia. Elife *3*, e02439.

Jessberger, S., Clark, R.E., Broadbent, N.J., Clemenson, G.D., Consiglio, A., Lie, D.C., Squire, L.R., and Gage, F.H. (2009). Dentate gyrus-specific knockdown of adult neurogenesis impairs spatial and object recognition memory in adult rats. Learn Mem. *16*, 147–154.

Jin, J.H., Deng, J.Z., Wang, F., Xia, X.Y., Qiu, T.F., Lu, W.B., Li, X.W., Zhang, H., Gu, X.Y., Liu, Y.G., et al. (2013). The expression and function of microRNA-203 in lung cancer. Tumor Biol. *34*, 349–357.

Kawahara, H., Imai, T., and Okano, H. (2012). MicroRNAs in neural stem cells and neurogenesis. Front Neurosci. *6*, 30.

Lie, D.C., Colamarino, S.A., Song, H.J., Desire, L., Mira, H., Consiglio, A., Lein, E.S., Jessberger, S., Lansford, H., Dearie, A.R., et al. (2005). Wnt signalling regulates adult hippocampal neurogenesis. Nature *437*, 1370–1375.

Lindvall, O., Kokaia, Z., and Martinez-Serrano, A. (2004). Stem cell therapy for human neurodegenerative disorders—how to make it work. Nat. Med. *10*, S42–S50.

Lindvall, O., Barker, R.A., Brustle, O., Isacson, O., and Svendsen, C.N. (2012). Clinical translation of stem cells in neurodegenerative disorders. Cell Stem Cell *10*, 151–155.

Liu, C., Teng, Z.Q., Santistevan, N.J., Szulwach, K.E., Guo, W., Jin, P., and Zhao, X. (2010). Epigenetic regulation of miR-184 by MBD1 governs neural stem cell proliferation and differentiation. Cell Stem Cell *6*, 433–444.

Liu, C., Teng, Z.Q., McQuate, A.L., Jobe, E.M., Christ, C.C., von Hoyningen-Huene, S.J., Reyes, M.D., Polich, E.D., Xing, Y., Li, Y., et al. (2013a). An epigenetic feedback regulatory loop involving microRNA-195 and MBD1 governs neural stem cell differentiation. PLoS One *8*, e51436.

Liu, C.M., Wang, R.Y., Saijilafu, Jiao, Z.X., Zhang, B.Y., and Zhou, F.Q. (2013b). MicroRNA-138 and SIRT1 form a mutual negative feedback loop to regulate mammalian axon regeneration. Genes Dev. *27*, 1473–1483.

Margueron, R., and Reinberg, D. (2011). The Polycomb complex PRC2 and its mark in life. Nature *469*, 343–349.

Margueron, R., Justin, N., Ohno, K., Sharpe, M.L., Son, J., Drury, W.J., 3rd, Voigt, P., Martin, S.R., Taylor, W.R., De Marco, V., et al. (2009). Role of the polycomb protein EED in the propagation of repressive histone marks. Nature *461*, 762–767.

Mohamed Ariff, I., Mitra, A., and Basu, A. (2012). Epigenetic regulation of self-renewal and fate determination in neural stem cells. J. Neurosci. Res. *90*, 529–539.

Molofsky, A.V., Pardal, R., Iwashita, T., Park, I.K., Clarke, M.F., and Morrison, S.J. (2003). *Bmi-1* dependence distinguishes neural stem cell self-renewal from progenitor proliferation. Nature *425*, 962–967.

Nakashima, K., Takizawa, T., Ochiai, W., Yanagisawa, M., Hisatsune, T., Nakafuku, M., Miyazono, K., Kishimoto, T., Kageyama, R., and Taga, T. (2001). BMP2-mediated alteration in the developmental pathway of fetal mouse brain cells from neurogenesis to astrocytogenesis. Proc. Natl. Acad. Sci. USA *98*, 5868–5873.

Nguyen, L.H., Diao, H.J., and Chew, S.Y. (2015). MicroRNAs and their potential therapeutic applications in neural tissue engineering. Adv. Drug Deliv. Rev. *88*, 53–66.

Nissan, X., Denis, J.A., Saidani, M., Lemaitre, G., Peschanski, M., and Baldeschi, C. (2011). miR-203 modulates epithelial differentiation of human embryonic stem cells towards epidermal stratification. Dev. Biol. *356*, 506–515.

Pereira, J.D., Sansom, S.N., Smith, J., Dobenecker, M.W., Tarakhovsky, A., and Livesey, F.J. (2010). *Ezh2*, the histone methyltransferase of PRC2, regulates the balance between self-renewal and differentiation in the cerebral cortex. Proc. Natl. Acad. Sci. USA *107*, 15957–15962.

Rivetti di Val Cervo, P., Lena, A.M., Nicoloso, M., Rossi, S., Mancini, M., Zhou, H., Saintigny, G., Dellambra, E., Odorisio, T., Mahe, C., et al. (2012). p63-microRNA feedback in keratinocyte senescence. Proc. Natl. Acad. Sci. USA *109*, 1133–1138.

Ru, P., Steele, R., Hsueh, E.C., and Ray, R.B. (2011). Anti-miR-203 upregulates SOCS3 expression in breast cancer cells and enhances cisplatin chemosensitivity. Genes Cancer *2*, 720–727.

Ruan, L.H., Lau, B.W.M., Wang, J.X., Huang, L.J., ZhuGe, Q.C., Wang, B., Jin, K.L., and So, K.F. (2014). Neurogenesis in neurological and psychiatric diseases and brain injury: from bench to bedside. Prog. Neurobiol. *115*, 116–137.

Shen, X.H., Liu, Y.C., Hsu, Y.J., Fujiwara, Y., Kim, J., Mao, X.H., Yuan, G.C., and Orkin, S.H. (2008). EZH1 mediates methylation on histone H3 lysine 27 and complements EZH2 in maintaining stem cell identity and executing pluripotency. Mol. Cell *32*, 491–502.

Sher, F., Rossler, R., Brouwer, N., Balasubramaniyan, V., Boddeke, E., and Copray, S. (2008). Differentiation of neural stem cells into oligodendrocytes: involvement of the polycomb group protein *Ezh2*. Stem Cells *26*, 2875–2883.

Silahtaroglu, A.N., Nolting, D., Dyrskjot, L., Berezikov, E., Moller, M., Tommerup, N., and Kauppinen, S. (2007). Detection of microRNAs in frozen tissue sections by fluorescence in situ hybridization using locked nucleic acid probes and tyramide signal amplification. Nat. Protoc. *2*, 2520–2528.

Spalding, K.L., Bergmann, O., Alkass, K., Bernard, S., Salehpour, M., Huttner, H.B., Bostrom, E., Westerlund, I., Vial, C., Buchholz, B.A.,

et al. (2013). Dynamics of hippocampal neurogenesis in adult humans. Cell *153*, 1219–1227.

Sparmann, A., and van Lohuizen, M. (2006). Polycomb silencers control cell fate, development and cancer. Nat. Rev. Cancer *6*, 846–856.

Stenudd, M., Sabelstrom, H., and Frisen, J. (2015). Role of endogenous neural stem cells in spinal cord injury and repair. JAMA Neurol. *72*, 235–237.

Szulwach, K.E., Li, X., Smrt, R.D., Li, Y., Luo, Y., Lin, L., Santistevan, N.J., Li, W., Zhao, X., and Jin, P. (2010). Cross talk between microRNA and epigenetic regulation in adult neurogenesis. J. Cell Biol. *189*, 127–141.

Takamatsu-Ichihara, E., and Kitabayashi, I. (2016). The roles of Polycomb group proteins in hematopoietic stem cells and hematological malignancies. Int. J. Hematol. *103*, 634.

Viticchie, G., Lena, A.M., Latina, A., Formosa, A., Gregersen, L.H., Lund, A.H., Bernardini, S., Mauriello, A., Miano, R., Spagnoli, L.G., et al. (2011). MiR-203 controls proliferation, migration and invasive potential of prostate cancer cell lines. Cell Cycle *10*, 1121–1131.

Wang, H.B., Wang, L.J., Erdjument-Bromage, H., Vidal, M., Tempst, P., Jones, R.S., and Zhang, Y. (2004). Role of histone H2A ubiquitination in polycomb silencing. Nature *431*, 873–878.

Yi, R., Poy, M.N., Stoffel, M., and Fuchs, E. (2008). A skin microRNA promotes differentiation by repressing 'stemness'. Nature *452*, 225–229.

Yonemitsu, Y., Imazeki, F., Chiba, T., Fukai, K., Nagai, Y., Miyagi, S., Arai, M., Aoki, R., Miyazaki, M., Nakatani, Y., et al. (2009). Distinct expression of polycomb group proteins EZH2 and BMI1 in hepatocellular carcinoma. Hum. Pathol. *40*, 1304–1311.

Yu, H.X., Simons, D.L., Segall, I., Carcamo-Cavazos, V., Schwartz, E.J., Yan, N., Zuckerman, N.S., Dirbas, F.M., Johnson, D.L., Holmes, S.P., et al. (2012). PRC2/EED-EZH2 complex is up-regulated in breast cancer lymph node metastasis compared to primary tumor and correlates with tumor proliferation in situ. PLoS One *7*, e51239.

Yu, X.Y., Jiang, X.R., Li, H.X., Guo, L.P., Jiang, W., and Lu, S.H. (2014). miR-203 inhibits the proliferation and self-renewal of esophageal cancer stem-like cells by suppressing stem renewal factor *Bmi-1*. Stem Cells Dev. *23*, 576–585.

Yu, J.H., Seo, J.H., Lee, J.Y., Lee, M.Y., and Cho, S.R. (2016). Induction of neurorestoration from endogenous stem cells. Cell Transplant. *25*, 863–882.

Zencak, D., Lingbeek, M., Kostic, C., Tekaya, M., Tanger, E., Hornfeld, D., Jaquet, M., Munier, F.L., Schorderet, D.F., van Lohuizen, M., et al. (2005). *Bmi1* loss produces an increase in astroglial cells and a decrease in neural stem cell population and proliferation. J. Neurosci. *25*, 5774–5783.

Zhang, J., Ji, F., Liu, Y., Lei, X., Li, H., Ji, G., Yuan, Z., and Jiao, J. (2014). Ezh2 regulates adult hippocampal neurogenesis and memory. J. Neurosci. *34*, 5184–5199.

Zhang, J., Taylor, R.J., La Torre, A., Wilken, M.S., Cox, K.E., Reh, T.A., and Vetter, M.L. (2015). *Ezh2* maintains retinal progenitor proliferation, transcriptional integrity, and the timing of late differentiation. Dev. Biol. *403*, 128–138.

Ziegler, A.N., Levison, S.W., and Wood, T.L. (2015). Insulin and IGF receptor signalling in neural-stem-cell homeostasis. Nat. Rev. Endocrinol. *11*, 161–170.